

Band structure calculations of CuAlO₂, CuGaO₂, CuInO₂, and CuCrO₂ by screened exchange

Roland Gillen* and John Robertson

Department of Engineering, University of Cambridge, Cambridge CB3 0FA, United Kingdom

(Received 21 January 2011; revised manuscript received 4 May 2011; published 26 July 2011)

We report density functional theory band structure calculations on the transparent conducting oxides CuAlO₂, CuGaO₂, CuInO₂, and CuCrO₂. The use of the hybrid functional screened-exchange local density approximation (sX-LDA) leads to considerably improved electronic properties compared to standard LDA and generalized gradient approximation (GGA) approaches. We show that the resulting electronic band gaps compare well with experimental values and previous quasiparticle calculations, and show the correct trends with respect to the atomic number of the cation (Al, Ga, In). The resulting energetic depths of Cu *d* and O *p* levels and the valence-band widths are considerable improvements compared to LDA and GGA and are in good agreement with available x-ray photoelectron spectroscopy data. Lastly, we show the calculated imaginary part of the dielectric function for all four systems.

DOI: 10.1103/PhysRevB.84.035125

PACS number(s): 71.20.-b, 78.20.-e, 71.15.-m

I. INTRODUCTION

“Invisible electronic devices,” which allow for novel flat panel systems and improved solar cells, are an interesting new field in optoelectronics. Such systems require transparent or nearly transparent materials with band gaps in the range of 3 eV or above and good *n*- and *p*-type dopability. Transparent conductive oxides (TCOs) are promising candidate materials and have excited intensive research during the previous decade for this reason. Good *n*-type dopability is achievable in ZnO, In₂O₃,^{1,2} and SnO₂,³ but *p*-type doping still is difficult. The tendency of oxides to form nonbonding O 2*p* states with a high effective mass at the valence-band maximum is problematic, as a low effective mass is needed for ionizable shallow acceptor states.⁴ In 1997, Kawazoe *et al.*⁴ reported *p*-type conductivity in combination with transparency in CuAlO₂ and similar properties were discovered for other members of the CuMO₂ (M = Ga, In, Cr, etc.) group. These materials possess inherent advantages over Cu₂O: (i) Their optical band gaps are 3 eV and above, and (ii) the additional cations M are likely to stabilize the oxygen atoms in the compound and contribute to dopability.⁵

Despite the many scientific reports on CuMO₂, details of the band structure and the electronic properties, such as hole conductivity mechanism and the abundance of compensating defects in these materials, are still unclear. Here, *ab initio* calculations are valuable. However, the common density functional theory (DFT) calculations within the local density approximation (LDA) or the generalized gradient approximation (GGA) lack the derivative discontinuity with respect to fractional charges⁶ and, thus, suffer from spurious self-interaction. This self-interaction promotes artificial delocalization of electron states and causes occupied states to be placed too high in energy, lowering the size of the predicted band gaps. This limits the predictive abilities of these approximations. It is thus necessary to go beyond LDA and GGA for the theoretical investigation of the electronic properties.

In this paper, we present calculations of the electronic properties of four delafossite TCOs (CuAlO₂, CuGaO₂, CuInO₂, and CuCrO₂) employing the screened-exchange-LDA (sX-LDA) hybrid functional.^{7,8} The inclusion of exact Hartree-Fock exchange compensates for the self-interaction

error and has a beneficial effect on the predicted electronic properties. (i) We show that sX-LDA noticeably improves on the band-gap energies compared to LDA and GGA for all studied TCOs and compare our values with those from other methods. (ii) The experimentally observed trend of the band gaps in the sequence CuAlO₂-CuGaO₂-CuInO₂ is reproduced by our sX-LDA calculations. (iii) The predicted valence-band widths (with possibly the exception of CuCrO₂) and (iv) the depths of the Cu *d* levels are close to experimental values. Further, we provide the calculated imaginary part of the dielectric function for all studied materials. We identify a strong renormalization of the *d*-state energy to be the main factor in our calculations.

II. METHOD

There are various methods to improve the band gaps. A widespread and computationally efficient approach is LDA + *U*,⁹ where an empirical on-site Coulomb energy is added to selected orbitals. The energetical downshift and upshift of the corresponding bands compared to pure LDA results in improved band gaps. Green's function approaches such as *GW* (Ref. 10) and its approximations¹¹ explicitly address the many-body problem and treat electrons as quasiparticles. The aim is then to calculate the electron self-energy in terms of the single-particle Green's function *G* and a dynamically screened Coulomb interaction *W*. While the resulting quasiparticle energies lead to accurate band gaps, the frequency- and energy-dependent screening in *W* makes the method computationally expensive.

An alternative is to include a fraction of screened Hartree-Fock exchange in otherwise purely density-dependent exchange-correlation functionals. The idea of such hybrid functionals is a best-of-both-worlds approach to solve the band-gap problem by combining the overestimation of band gaps from Hartree-Fock with the underestimation from LDA and GGA. Heyd, Scuseria, and Ernzerhof¹² (HSE) is such a functional, which recently gained large popularity. It yields good results for small and medium band-gap semiconductors.

In this paper, we use the hybrid functional sX-LDA. The sX-LDA method was proposed by Bylander and Kleinman⁷ as a modification of the local density approximation on empirical

grounds. Seidl *et al.* later showed that the method can be derived from a generalized Kohn-Sham scheme. The idea is to split the exchange-correlation potential in (i) an orbital-dependent short-range term, which can be treated exactly, and (ii) an explicit density functional term for long-range exchange in order to recover the accurate LDA behavior for homogeneous electron gases. The exchange-correlation (XC) potential can then be written as

$$V_{XC}^{sX-LDA} = V_x^{sX} + V_{XC}^{LDA} - V_x^{sX,local} \quad (1)$$

and describes the exchange interaction by a statically screened exact-exchange term

$$V_x^{sX} = \sum_{i,j} \int d\mathbf{r} \frac{\psi_i^*(\mathbf{r}) e^{k_s |\mathbf{r}-\mathbf{r}'|} \psi_j(\mathbf{r})}{|\mathbf{r}-\mathbf{r}'|}, \quad (2)$$

usually with the Thomas-Fermi (TF) wave vector $k_s = k_{TF} = 2[\frac{3}{\pi}\rho]^{1/6}$ as inverse screening length. While the TF screening length yields reasonable results for s - p semiconductors, it apparently overestimates the electronic screening in case transition metals are involved. An empirical value of $k_s = 0.5$ reproduces the experimental band gaps of various transition-metal compounds, such as GaN, MnO, and NiO, with similar average densities ρ as our studied TCOs. Due to the weak density dependence of the Thomas-Fermi wave vector, we chose to use this value for our calculations on the CuMO₂ series as well.

The sX-LDA method has recently¹³ been implemented within the plane-wave basis set in the DFT package CASTEP (Ref. 14) and was shown to yield band gaps that usually can compete in accuracy with those from G_0W_0 . The potential of the ions was modeled by OPIUM-generated norm-conserving pseudopotentials and the electrons were represented by plane waves with a cutoff energy of 800 eV for all structures. We averaged the integration over reciprocal space using a grid of $4 \times 4 \times 4$ evenly distributed k points in the Brillouin zone. The PW91 and sX-LDA band structures were obtained by ground-state minimization and subsequent band structure calculation, with the exception of CuCrO₂, where we had to obtain the sX-LDA band structure by perturbation of the spin-polarized PW91 ground state for speed reasons.

CuMO₂ TCOs crystallize in the delafossite structure, consisting of planes of O atoms caged in tetrahedra made of M anions and Cu atoms. The planes are connected by dumbbell-like O-Cu-O bridges. Depending on whether the layer stacking is AB or ABC, the structure is of the $2H$ type with hexagonal $P6_3/mmm$ symmetry, or of the $3R$ type with rhombohedral $R\bar{3}m$ symmetry. The energy difference between both structures is low. We thus modeled our studied TCOs by a rhombohedral unit cell with the lattice vectors $a_1 = (\frac{a}{2}, -2\sqrt{3}a, \frac{c}{3})$, $a_2 = (-\frac{a}{2}, -2\sqrt{3}a, \frac{c}{3})$, $a_3 = (0, 2\sqrt{3}a, \frac{c}{3})$ atoms at the Wyckoff positions Cu: (0,0,0), M: ($\frac{1}{2}, \frac{1}{2}, \frac{1}{2}$), O: $\pm (z, z, z)$, where a and c are the lattice constants of the nonprimitive hexagonal unit cell of the $3R$ -type crystal and z the Cu-O distance.

A test-wise optimization of the cell parameters of CuAlO₂ showed a very small change of 0.7% compared to the lattice parameters and we decided to use the experimental values for all our calculations in order to be consistent with calculations from other groups. On this basis, we relaxed the

atomic positions until the residual forces were smaller than 10^{-3} eV/Å. We further used a grid of $10 \times 10 \times 10$ equidistant points in the Brillouin zone for the calculations of the optical properties and the density of states.

III. RESULTS AND DISCUSSION

A. Band structures of CuAlO₂, CuGaO₂, and CuInO₂

We start our discussion with CuAlO₂, certainly the most prominent delafossite material. Available experimental values for the optical band gaps of CuAlO₂ are quite disperse and range between 2.9 (Ref. 15) and 3.9 (Ref. 16) eV, where most studies point to a gap of 3.5–3.6 eV.^{4,17,18} Theoretical studies point toward the existence of an indirect fundamental band gap, which forms a tail of weak absorption below the optical band gap.¹⁹ Evidence for such an indirect band gap was found experimentally, although the band-gap size is subject to debate: Various experimental studies^{17,20} on CuAlO₂ located an indirect band gap at 1.6–1.8 eV, i.e., far below the optical band gap. Based on accurate hybrid functional calculations, Scanlon *et al.* proposed that these results might in fact arise from deep defect levels in the band gap from Cu_{Al} antisites.²¹ Indeed, more recent studies²² on thicker films suggested a value of around 3 eV for the indirect transition.

Figure 1(a) shows the band structure of CuAlO₂ from our sX-LDA calculations in comparison to those from GGA. The Cu atoms introduce shallow $3d$ electrons, which are energetically degenerate with the weakly dispersive states from nonbonding O $2p$ orbitals and dominate the upper valence band. Interaction of Cu $3d$ and O states locally push up a mixed Cu-O state above the undispersed background and form a mesa between the valence-band maximum at the F point and an energetically slightly lower extremum at L . The lower effective mass of this state supports the formation of shallow acceptor levels. The lowest conduction band shows a marked dispersion with local minima of the conduction band

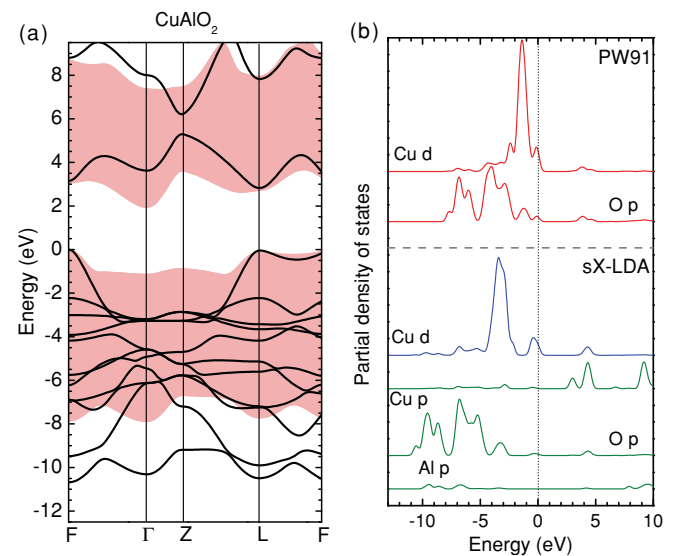


FIG. 1. (Color online) (a) Electronic band structures of CuAlO₂ from sX-LDA (black solid lines) and GGA (shaded area) calculations. (b) Corresponding partial density of states of the dominant angular momentum channels.

at or near all high-symmetry points. GGA, as well as the hybrid functionals B3LYP (Ref. 23) and HSE (Refs. 21,24 and 25), and also G_0W_0 ,^{24,25} predict the global conduction-band minimum to be at the Γ point, with a rivaling minimum at the L point. A previous study using the sX functional (i.e., Thomas-Fermi screened Hartree-Fock exchange) yielded the same result,²⁶ but underestimated the band gap due to using a larger inverse screening length k_s for the calculation of the screened Hartree-Fock contribution.

The situation is clearly different in our sX-LDA band structure. Here, the renormalization at the high-symmetry points is remarkably dependent on the contribution of different states to the local band structure. Inclusion of nonlocal exchange affected particularly the lowest conduction band at the Γ and the Z point, which are dominated by Cu d and s states with contributions of O p (Z) and Al p (Γ). In contrast, the conduction band at the F and the L points consists of Cu p states mixed with Al s (L) and O p (F) and these states experienced only a small renormalization of 0.3 eV. As a consequence, the minimum at the Γ point is pushed above the minima at L and F points, the global conduction-band minimum moves to the L point. We find a minimum indirect band gap of 2.8 eV between the F and the L points and a slightly larger direct band gap of 2.95 eV at the L point. The qualitative prediction of the lowest conduction band in our case is very similar to the band structure from self-consistent quasiparticle G_0W_0 @scCOHSEX calculations, as reported recently by Trani *et al.*²⁵ The reason might be the similar description of statically screened-exchange interaction in sX-LDA and COHSEX, which is different to the (screened) exact exchange portions in HSE and B3LYP. Table I summarizes the indirect and direct band gaps as obtained by the different methods.

The valence band draws a similar picture to the conduction band. The lifting of self-interaction causes a strong downward push of the Cu d and O p dominated high-mass bands at the valence-band top and leaves a high mesa between the valence-band maximum (VBM) and the L point. This opens the direct band gap at the Γ point to a value of 6.8 eV. The valence Cu d states give rise to a high peak in the partial density of states (PDOS) [Fig. 1(b)], which is shifted down by 1.8 eV compared to GGA. We find the peak maximum at about 3.1 eV and an additional shoulder at about 2.9–3 eV below the VBM. Interestingly, this agrees well with recent x-ray

photoelectron spectroscopy (XPS) experiments,^{27,28} where the peak maximum was found at an energy of -2.8 to -3 eV. The good prediction of the depth of d levels from sX-LDA was previously shown for ZnO and other transition-metal semiconductors.^{29,30}

A characteristic effect of nonlocal exchange in isolated atoms is the species-dependent renormalization of energy levels from the lifted self-interaction. To a certain extent, this carries over to solids and manifests in a change of electron negativity difference, the lowering in energy levels, and the broadening of the energy spectra. For CuAlO₂, we observe a transfer of charge from the aluminium ions to the oxygen cations, which leads to a slight increase in bond polarization and might be responsible for the opening of the band gap. The PDOS suggests a strong energetic downshift and broadening of oxygen and aluminium states. The oxygen $2p$ states are shifted down by 2 eV compared to GGA and broadened down to an energy of 11 eV below the valence-band maximum. This nicely agrees with available experimental XPS data.²⁷

In the optical spectra, replacing Al by heavier group-III atoms such as Ga or In seems to shift the onset of optical absorption to higher energies. The reported optical band gaps for CuGaO₂ and CuInO₂ are 3.6 eV (Ref. 32) and 3.9 eV,³³ respectively, whereas the direct gap in CuAlO₂ is controversial but likely around 3.5 eV. At first glance, this seems to contradict the trend in other oxides, where the optical band gap decreases with the atomic number. Based on linearized augmented plane-wave (LAPW) LDA calculations, Nie *et al.*¹⁹ suggested that the observed absorption onset corresponds not to the minimum band gaps but to direct optical transitions at the L point, as the direct transitions at the Γ and Z points are symmetry forbidden. Indeed, GGA band structures for CuGaO₂ and CuInO₂ show that the conduction-band minimum at the Γ point moves toward lower energies for increasing atomic number. This is due to the contribution of antibonding s states at these points, which become energetically more favorable as the volume of the unit cell increases. On the other hand, the local conduction-band minimum near the L point smoothens and becomes less prominent, thus, effectively increasing the optically active direct gap at the L point. Previous hybrid functional and GW calculations predicted a noticeable change in dispersion at the valence-band top compared to LDA and GGA owing to the lower energy of the low-mass Cu d bands. As a result, the minimum direct band gaps for CuGaO₂ and CuInO₂ shift from the Γ point to the L point. We find the same behavior in our sX-LDA calculations [see Figs. 2(a) and 2(b)]. While the different renormalization of points with and without d contributions narrows the lowest conduction band, the minima at the L and F points become more prominent and preferable points for optical transitions.

Figure 3 compares the calculated direct and indirect band gaps at the L point from different methods. Our calculated band gap for CuInO₂ of 3.8 eV compares nicely with the experimentally measured optical band gap of 3.9 eV, with only G_0W_0 being closer. HSE06 and G_0W_0 @scCOHSEX overestimate the band gap, while GGA, as expected, underestimates. The available results for CuGaO₂ are less favorable. Trani *et al.*²⁵ reported that G_0W_0 @scCOHSEX gives a band-gap size smaller than that in CuAlO₂, thus breaking the trend of the predicted

TABLE I. Calculated band gaps in CuAlO₂ from GGA, various hybrid functionals, and quasiparticle calculations. sc G_0W_0 (+ P) refers to G_0W_0 @scCOHSEX (calculations with model polaron correction). The minimum band gap is indirect in all methods.

Method	E_{ind} (eV)	E_{dir} (L point) (eV)
PW91	1.9	2.6
B3LYP (Ref. 23)	3.9	4.5
HSE06 (Ref. 25)	3.6	4.1
sX-LDA	2.8	2.95
G_0W_0 (Ref. 25)	3.1	3.4
sc G_0W_0 (Ref. 25)	5.0	5.1
sc G_0W_0 + P (Ref. 25)	3.8	3.9
Experiment	3.0	3.5

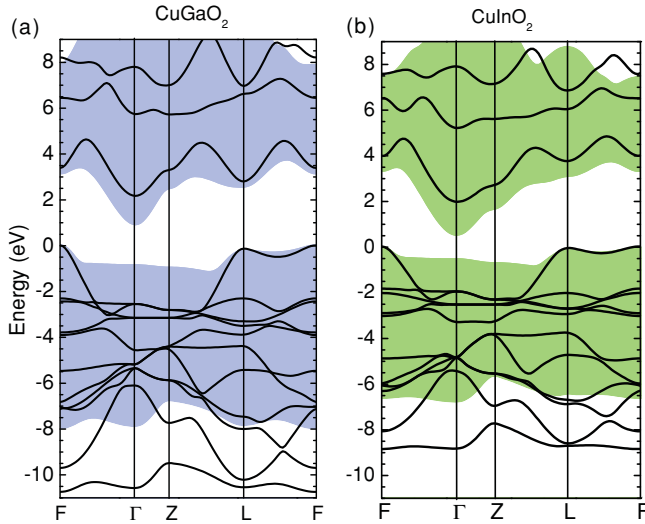


FIG. 2. (Color online) Comparison of sX-LDA band structures of (a) CuGaO_2 and (b) CuInO_2 . The shaded areas represent the valence and conduction bands from GGA calculations.

optical band gaps to increase with the atomic mass. Similarly, the value from our sX-LDA calculations is almost identical to the band gap in CuAlO_2 . In case of indirect band gaps [Fig. 3(b)], all methods predict a noticeable decrease in band-gap size with atomic weight. Sasaki *et al.*³⁴ found for CuInO_2 an indirect band of 1.44 eV, in sight of the predicted band gaps from G_0W_0 , sX-LDA, HSE, and even B3LYP. As suggested for CuAlO_2 , deep defect levels or excitons might lead to a shift of the measured indirect band gap toward lower energies.

Similar to the indirect band gap, the valence-band width also exhibits a decreasing trend in the sequence $\text{CuAlO}_2 > \text{CuGaO}_2 > \text{CuInO}_2$, which roots in the increase in Cu-O bond lengths.³¹ GGA reproduces the trend but compresses the valence bands of all three materials by several electronvolts (see Table II). Our sX-LDA calculations show an appreciable improvement in the absolute values, which are close to the experimentally obtained bandwidths in the range 9–11 eV.

Finally, we have performed optical calculations within sX-LDA on the three systems. Figure 4(a)-4(c) shows the obtained imaginary part of the dielectric functions for light

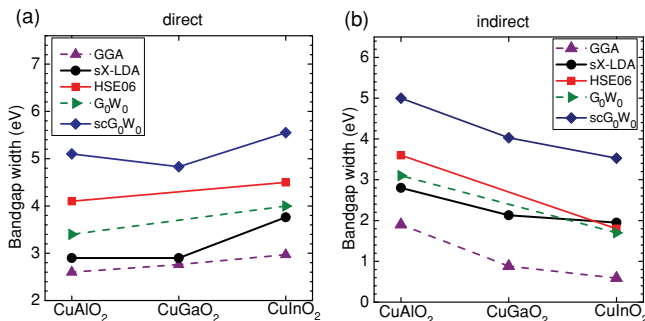


FIG. 3. (Color online) Trends of fundamental (a) direct and (b) indirect band gaps of CuMO_2 ($M = \text{Al, Ga, In}$) with the atomic mass of M . For brevity, $\text{sc}G_0W_0$ refers to G_0W_0 @ scCOHSEX .

TABLE II. Valence-band widths as obtained from GGA, sX-LDA, and experiments.

Approximation	CuAlO_2 (eV)	CuGaO_2 (eV)	CuInO_2 (eV)
GGA	8	8	7
sX-LDA	10.75	10.7	9
Experiment (Ref. 31)	11	10	9.5

polarized parallel and perpendicularly to the c axis of the crystal. In accordance to the absorption spectra from Nie *et al.*,¹⁹ we observe a noticeable anisotropy with respect to the light polarization. As the absorption coefficient is proportional to $\text{Im}(\epsilon)$, significant absorption of light polarization along the layer stacking is retarded toward higher energies, with a tail reaching down to the optical band-gap energy. The onset of appreciable absorption is located at an energy of 3–4 eV for all materials, confirming that transitions involving the Γ and Z points provide no, or only a small, contribution to the low-energy absorption. At the same time, these values fit well to the direct transitions around the L and F points. We further used the calculated dielectric functions to calculate the absorption onset of the three systems by means of Tauc's plots. Indeed, the obtained absorption edges for direct transitions are in very good agreement with the fundamental direct gaps at the L point, see Fig. 4(d).

B. Band structure of CuCrO_2

Another group of Cu-based transparent conducting oxides contains particular transition metals, e.g., Fe or Cr, instead

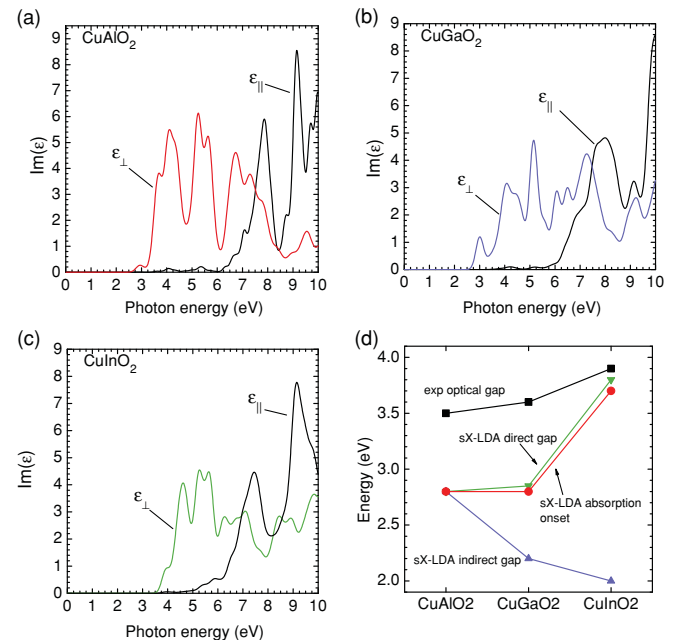


FIG. 4. (Color online) Imaginary part of the dielectric function for light polarized parallel (ϵ_{\parallel}) and perpendicular (ϵ_{\perp}) to the c axis from sX-LDA calculations on (a) CuAlO_2 , (b) CuGaO_2 , and (c) CuInO_2 . The peaks were broadened by a Gaussian smearing of 0.1 eV. (d) Comparison of the absorption onsets (circles), as obtained by plotting α $h\nu$ - $h\nu$ curves, with experimental optical band gaps (squares) and fundamental direct and indirect transitions (triangles).

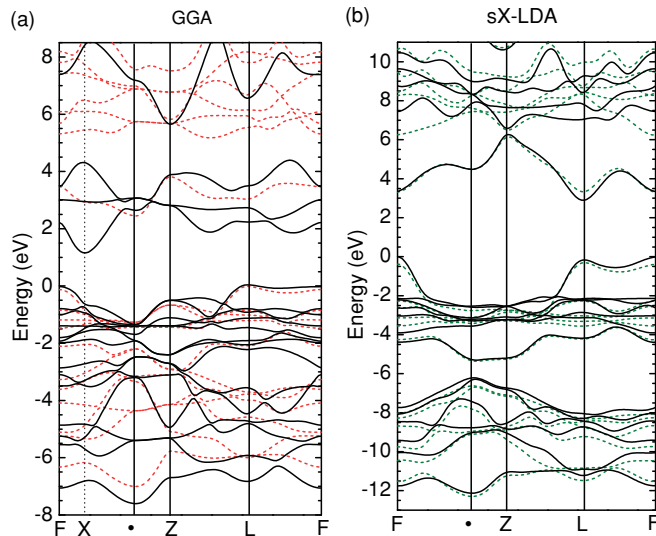


FIG. 5. (Color online) Electronic band structures from (a) GGA and (b) sX-LDA calculations. The black solid lines and the broken lines represent states of up-spin and down-spin direction electrons, respectively.

of elements from the third group. The electrons in the partly filled d orbitals might then form a magnetic order and thus allow for transparent materials with magnetic properties. Aside from magnetic properties, Mg-doped CuCrO_2 possesses the highest conductivity of all reported delafossites.³⁵ Studies on CuCrO_2 found an absorption onset energy of about 3 eV,^{36,37} which renders CuCrO_2 to be transparent, and additional indirect transitions at 1.28 (Ref. 36) and 1.45 eV.³⁸ The nature of the optical transition at 3 eV is not fully clear. Early photoelectrochemical measurements³⁶ suggest an indirect gap, whereas recent absorption measurements point toward a direct transition.

We have calculated the ground state and the electronic band structure for CuCrO_2 by means of GGA and sX-LDA. The Cr atoms are spin polarized and impose an antiferromagnetic order on the ground state of the crystal, which we confirmed on a $2 \times 2 \times 2$ rhombohedral supercell. The energy difference between antiferromagnetic and ferromagnetic spin order, however, was found to be of order 1 meV, so we chose to model CuCrO_2 by the rhombohedral unit cell in our calculations to save computational resources. Figure 5(a) shows the band structure of CuCrO_2 from GGA calculations. Due to the ferromagnetic ground state, three occupied single electron Cr d states appear close to the valence band top, whereas the two remaining two, unoccupied, alpha-spin Cd d states constitute

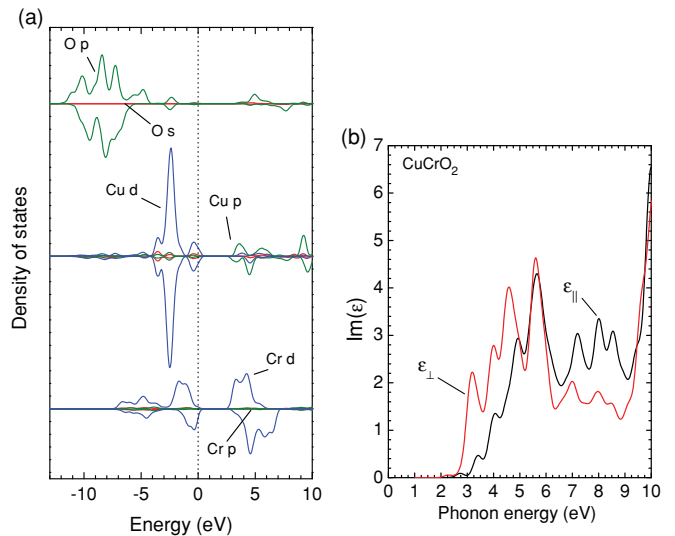


FIG. 6. (Color online) (a) Partial density of states and (b) imaginary part of the dielectric function of CuCrO_2 from sX-LDA calculations. The peaks were broadened by a Gaussian smearing of 0.1 eV.

the bottom of the conduction band. The complementary β -spin bands are shifted deep in the conduction band due to the exchange splitting. The global conduction-band minimum of 1.12 eV is located between the F and the Γ points, the fundamental band gap being indirect and between this point (X point) and the F point. The minimum direct gap of 1.97 eV is at the X point and differs from the indirect band gap by the difference in the valence-band top. The qualitative positions of the fundamental transitions are in good agreement with the band structures of Scanlon *et al.*,²⁸ who used a hexagonal $2H$ unit cell and GGA+ U to simulate CuCrO_2 and obtained an antiferromagnetic ground state.

Screened exact exchange noticeably changes the predicted band structure [see Fig. 5(b)]. In general, the respective band structures of α - and β -spin electrons become quite similar, in contrast to the GGA. As for the other CuMO_2 , the energies at the d -state dominated Γ and Z points are strongly shifted up and the global minimum moves to the L point, with a rivaling distinctive minimum appearing at the F point. As a consequence, the indirect band gap opens to 2.9 eV and is between the F and L points, the minimum direct band gap is 3.1 eV and at the L point. Another direct band gap occurs at the F point and is 3.25-eV wide. Scanlon *et al.*²⁸ report a value of 2.04 eV for the fundamental (indirect) gap, but find a larger difference between indirect and direct gaps due

TABLE III. Minimum indirect and direct band gaps of CuCrO_2 as obtained from GGA, GGA+ U , and sX-LDA calculations and experiments.

	E_{ind} (eV)	E_{dir} (L point) (eV)
GGA	1.12	1.97
GGA+ U (Ref. 28)	2.04	2.55
sX-LDA	2.9	3.1
Experiment	1.28 (Ref. 36), 1.45 (Ref. 38) 3.08 (Ref. 36)	3.1 (Ref. 36)

to the comparatively weak pushdown of the Cu d states in their calculations. Table III summarizes the obtained band-gap sizes. As a downside, the agreement of the valence-band width with experiment in sX-LDA is worse than in GGA. Arnold *et al.*³⁹ have reported a value of 8.2 eV for the valence-band width of CuCrO₂, which is a considerably lower value than would be expected from the Cu-O bond length. GGA captures this value quite well, whereas sX-LDA give a width of 12 eV [refer to the PDOS in Fig. 6(a)].

Finally, Fig. 6(b) shows the imaginary part of the dielectric function for light polarized perpendicularly and parallel to the c axis. The anisotropy as observed for the other systems is present but much less pronounced. This indicates a fairly homogeneous polarizability of CuCrO₂ within, and perpendicular to, the Cr-O layers.

IV. CONCLUSION

To summarize, we have used the screened-exchange hybrid functional sX-LDA to calculate the electronic and optical properties of various delafossite CuMO₂-type semiconductors ($M = \text{Al, Ga, In, Cr}$). A number of groups have previously reported studies on these materials with different methods. Local XC functionals (LDA, GGA) predict all four materials to be indirect semiconductors with a fundamental gap between the F and the Γ points.^{17,19} Nie *et al.*¹⁹ used symmetry arguments to show that the experimentally observed optical direct band gaps correspond to transitions at the L point. Local functionals systematically underestimate these transition energies as well as valence-band widths of the binding energies of the Cu d electrons due to severe self-interaction. Inclusion of nonlocal [LDA + U ,^{25,40} B3LYP,²³ HSE03,²⁵ and HSE06 (Refs. 21 and 25)] exchange or many-body effects (G_0W_0) (Ref. 25) does amend for these shortcomings and was shown to mainly induce a rigid shift on the conduction band to higher energies

and the flat Cu d at the valence-band top to lower energies. The resulting fundamental indirect and direct band gaps are considerably improved, whereas the binding energy of the d electrons still is considerably underestimated compared to XPS data. For CuAlO₂, Trani *et al.*^{24,25} recently reported that using a G_0W_0 @scCOHSEX approach yields a qualitatively different picture compared to the common methods. Here, the scCOHSEX ground state leads to a strong renormalization of the conduction bands in addition to a significant rigid shift. The local conduction-band minimum at the Γ point is pushed energetically above the local minimum at the L point, which becomes the new global minimum. This fits to the ongoing debate about the nature of the experimentally measured indirect band gap in CuAlO₂. However, G_0W_0 @scCOHSEX considerably overestimates the conduction-band energies and does not reproduce the experimental trends in the direct band gaps in the series CuAlO₂-CuGaO₂-CuInO₂.

Our sX-LDA calculations yield qualitatively similar results to G_0W_0 @scCOHSEX, but underestimate band gaps compared to experiments. On the other hand, valence-band widths and the binding levels of localized electrons (Cu d and O p) are in good agreement with experiments, the latter being significantly lower in energy than the d levels in corresponding calculations employing other functionals. For CuCrO₂, sX-LDA is very successful in reproducing the experimentally measured values for both the indirect and direct band gaps and shows big improvement over available GGA+ U calculations.²⁸ We further showed the calculated imaginary part of the dielectric function for all four studies' materials.

ACKNOWLEDGMENT

This work was supported by funds from the EU project Orama.

*rg403@cam.ac.uk

¹H. Hosono, *J. Non-Cryst. Solids* **352**, 851 (2006).
²K. Nomura, A. Takagi, T. Kamiya, H. Ohta, M. Hirano, and H. Hosono, *Jpn. J. Appl. Phys.* **45**, 4303 (2006).
³J. Robertson, *Phys. Status Solidi B* **245**, 1026 (2008).
⁴H. Kawazoe, M. Yasukawa, H. Hyodo, M. Kurita, H. Yanagi, and H. Hosono, *Nature (London)* **389**, 939 (1997).
⁵J. Robertson and S. Clark **83**, 072505 (2011).
⁶A. J. Cohen, P. Mori-Sanchez, and W. Yang, *Science* **321**, 792 (2008).
⁷D. M. Bylander and L. Kleinman, *Phys. Rev. B* **41**, 7868 (1990).
⁸A. Seidl, A. Görling, P. Vogl, J. A. Majewski, and M. Levy, *Phys. Rev. B* **53**, 3764 (1996).
⁹V. I. Anisimov, J. Zaanen, and O. K. Andersen, *Phys. Rev. B* **44**, 943 (1991).
¹⁰L. Hedin, *Phys. Rev.* **139**, A796 (1965).
¹¹F. Aryasetiawan and O. Gunnarsson, *Rep. Prog. Phys.* **61**, 237 (1998).
¹²J. Heyd, G. E. Scuseria, and M. Ernzerhof, *J. Chem. Phys.* **118**, 8207 (2003).

¹³S. J. Clark and J. Robertson, *Phys. Rev. B* **82**, 085208 (2010).
¹⁴M. D. Segall, P. J. D. Lindan, M. J. Probert, C. J. Pickard, P. J. Hasnip, S. J. Clark, and M. C. Payne, *J. Phys. Condens. Matter* **14**, 2717 (2002).
¹⁵R.-S. Yu, S.-C. Liang, C.-J. Lu, D.-C. Tasi, and F.-S. Shieua, *Appl. Phys. Lett.* **90**, 191117 (2007).
¹⁶A. N. Banerjee and K. K. Chattopadhyay, *J. Appl. Phys.* **97**, 084308 (2005).
¹⁷H. Yanagi, S. Inoue, K. Ueda, H. Kawazoe, H. Hosono, and N. Hamada, *J. Appl. Phys.* **88**, 4159 (2000).
¹⁸J. Tate, H. L. Ju, J. C. Moon, A. Zakutayev, A. P. Richard, J. Russell, and D. H. McIntyre, *Phys. Rev. B* **80**, 165206 (2009).
¹⁹X. Nie, S.-H. Wei, and S. B. Zhang, *Phys. Rev. Lett.* **88**, 066405 (2002).
²⁰F. A. Benko and F. P. Kottlyberg, *J. Phys. Chem. Solids* **45**, 57 (1984).
²¹D. O. Scanlon and G. W. Watson, *J. Phys. Chem. Lett.* **1**, 3195 (2010).
²²S. Gilliland, J. Pellicer-Porres, A. Segura, A. Munoz, P. Rodriguez-Hernandez, D. Kim, M. S. Lee, and T. Y. Kim, *Phys. Status Solidi B* **244**, 309 (2007).

- ²³J. Robertson, P. Peacock, M. D. Towler, and R. Needs, *Thin Solid Films* **411**, 96 (2001).
- ²⁴J. Vidal, F. Trani, F. Bruneval, M. A. L. Marques, and S. Botti, *Phys. Rev. Lett.* **104**, 136401 (2010).
- ²⁵F. Trani, J. Vidal, S. Botti, and M. A. L. Marques, *Phys. Rev. B* **82**, 085115 (2010).
- ²⁶J. Robertson, K. Xiong, and S. J. Clark, *Phys. Status Solidi B* **243**, 2054 (2006).
- ²⁷D. J. Aston, D. J. Payne, A. J. H. Green, R. G. Egdell, D. S. L. Law, J. Guo, P. A. Glans, T. Learmonth, and K. E. Smith, *Phys. Rev. B* **72**, 195115 (2005).
- ²⁸D. O. Scanlon, A. Walsh, B. J. Morgan, G. W. Watson, D. J. Payne, and R. G. Egdell, *Phys. Rev. B* **79**, 035101 (2009).
- ²⁹B. Lee, L.-W. Wang, and A. Canning, *J. Appl. Phys.* **103**, 113713 (2008).
- ³⁰S. J. Clark, J. Robertson, S. Lany, and A. Zunger, *Phys. Rev. B* **81**, 115311 (2010).
- ³¹D. Shin, J. S. Foord, D. J. Payne, T. Arnold, D. J. Aston, R. G. Egdell, K. G. Godinho, D. O. Scanlon, B. J. Morgan, G. W. Watson, E. Mugnier, C. Yaicle, A. Rougier, L. Colakerol, P. A. Glans, L. F. J. Piper, and K. E. Smith, *Phys. Rev. B* **80**, 233105 (2009).
- ³²K. Ueda, T. Hase, H. Yanagi, H. Kawazoe, H. Hosono, H. Ohta, M. Orita, and M. Hirano, *J. Appl. Phys.* **89**, 1790 (2001).
- ³³H. Yanagi, T. Hase, S. Ibuki, K. Ueda, and H. Hosono, *Appl. Phys. Lett.* **78**, 1583 (2001).
- ³⁴M. Sasaki and M. Shimode, *J. Phys. Chem. Solids* **64**, 1675 (2003).
- ³⁵J. Tate, M. Jayaraj, A. Draeseke, T. Ulbrich, A. Sleight, K. Vanaja, R. Nagarajan, J. Wager, and R. Hoffman, *Thin Solid Films* **411**, 119 (2002).
- ³⁶F. A. Benko and F. P. Koffyberg, *Mater. Res. Bull.* **21**, 753 (1986).
- ³⁷R. Nagarajan, A. D. Draeseke, A. W. Sleight, and J. Tate, *J. Appl. Phys.* **89**, 8022 (2001).
- ³⁸S. Y. Zheng, G. S. Jiang, J. R. Su, and C. F. Zhu, *Mater. Lett.* **60**, 3871 (2006).
- ³⁹T. Arnold, D. J. Payne, A. Bourlange, J. P. Hu, R. G. Egdell, L. F. J. Piper, L. Colakerol, A. DeMasi, P.-A. Glans, T. Learmonth, K. E. Smith, J. Guo, D. O. Scanlon, A. Walsh, B. J. Morgan, and G. W. Watson, *Phys. Rev. B* **79**, 075102 (2009).
- ⁴⁰N. E. Christensen, A. Svane, R. Laskowski, B. Palanivel, P. Modak, A. N. Chantis, M. van Schilfhaarde, and T. Kotani, *Phys. Rev. B* **81**, 045203 (2010).